Regular Article

PHYSICAL CHEMISTRY RESEARCH
Published by the
Iranian Chemical Society
www.physchemres.org
info@physchemres.org

Phys. Chem. Res., Vol. 12, No. 4, 991-1004, December 2024
DOI: 10.22036/pcr.2024.453866.2518

Evaluation of Designed Peptide Inhibitors in Destabilization of Aβ42 Protofibrils: A Molecular Dynamics Study

E. Zarurati and S. Jalili*

Department of Chemistry, K. N. Toosi University of Technology, P. O. Box: 15875-4416, Tehran, Iran

(Received 23 April 2024, Accepted 31 July 2024)

The development of Alzheimer's disease (AD), the most prevalent form of dementia, is associated with the abnormal aggregation of Amyloid-β (Aβ) peptides into fibrils and plaques, leading to a decline in brain function. A promising approach to treating Aβ pathology involves inhibiting fibrillogenesis and developing compounds that effectively disrupt the stable structure of Aβ fibrils. To investigate the destabilizing effects of peptides on Aβ42 protofibrils, we designed 42 different N-methylated peptides that bind to Aβ42 protofibrils. We then studied the protofibril-peptide interactions using molecular docking, free energy calculations, and molecular dynamics (MD) simulations. Our results demonstrate that peptides induce changes in the secondary structure of Aβ42 protofibrils, ultimately leading to the formation of a less ordered structure. Increased Root Mean Square Deviation (RMSD), reduced residue contacts, disrupted salt bridge interactions, and decreased hydrogen bonds between chains in the Aβ42 protofibril indicate destabilization of the protofibril structure. Among the peptides tested, **P3** and **P11**, both singly N-methylated, exhibited the most potential for disrupting the Aβ42 protofibril structure.

Keywords: Alzheimer's disease, Amyloid-β42 (Aβ42) protofibril, Molecular dynamics (MD) simulation, N-methylated peptides

INTRODUCTION

Alzheimer's is a fatal neurodegenerative disease that is associated with cognitive disorders such as deficits in memory, speech, behavior, and motor function. It appears as a gradual decrease in the higher functions of the brain and eventually leads to death [1,2]. The main hallmarks of the neuropathology of Alzheimer's disease (AD) include two major types of protein aggregates: intracellular neurofibrillary tangles of hyperphosphorylated tau protein and extracellular aggregates of amyloid-β (Aβ) peptide, also known as senile plaques [3,4]. Aβ is produced through proteolytic cleavage of amyloid precursor protein (APP) by β- and γ-secretase enzymes. APP is a transmembrane glycoprotein consisting of a cytoplasmic domain with 55 amino acids and a long extracellular domain containing 590-680 amino acids [4,5]. Depending on the position of cleavage on APP, there are several isoforms of Aβ with different sizes of 38-43 amino acids, the most prevalent of which are Aβ1–40 and Aβ1–42 (also named Aβ40 and Aβ42). Aβ42 is highly neurotoxic and has faster aggregation kinetics compared to Aβ40 [6-8]. The formation of Aβ peptide aggregates plays an essential role in the emergence and progression of Alzheimer's disease [7-9]. In the brains of Alzheimer's patients, Aβ peptides aggregate and turn into toxic oligomers. Non-covalent interactions between oligomers form protofibrils, which mature into amyloid-like fibrils, followed by filament aggregates, leading to the deposition of amyloid plaques. These plaques are hypothesized to contribute to neurodegeneration [4,6-8]. Several treatment approaches, including β-secretase inhibition, α-helix conformation stabilization, and aggregation inhibition, have been proposed to alter the disease progression [5,8,10].

The Aβ42 protofibril structure consists of five identical Leu17-Ala42 peptide chains, labeled as chains A-E. Each chain consists of two β-strands, β1 (Leu17-Ser26) and β2 (Ile31-Ala42), connected by a bend region (Asn27-Ala30). Interactions within and between Aβ chains stabilize the U-

*Corresponding author. E-mail: sjalili@kntu.ac.ir

shaped structure of Aβ protofibrils [11,12]. Several chemical compounds and peptide fragments based on the Aβ sequence have been explored to interfere with the Aβ aggregation process, raising hopes for the treatment of this disease. However, using unmodified peptides as therapeutic agents is challenging due to their low metabolic stability, poor membrane permeability, and limited ability to cross the blood-brain barrier [2,4,8,12]. Nevertheless, utilizing peptide derivatives and peptidomimetics to prevent protein-protein interactions (PPIs) is of particular importance to overcome these obstacles.

Several peptide modification methods have been reported to alter peptide sequences, including a combination of unnatural amino acids, peptides with D-amino acid residues, methylation, and amination of nitrogen amide [2,11,13-18]. Peptides containing N-methylated amino acids have been identified as promising agents for blocking PPIs involving β-rich interactions [19-23]. In an experimental study, Schwartz et al. showed that among the two types of modifications in the peptide backbone, N-methylation can significantly impair Aβ fibrillation [24]. In the present investigation, we have chosen the Aβ29-37 hydrophobic fragment of the Aβ peptide for the design of inhibitors. A series of N-methylated peptides were designed, and their destabilizing effect on the Aβ42 protofibril was investigated using various computational methods.

COMPUTATIONAL DETAILS

Design of Candidate Peptides

The hydrophobic sequence of Aβ29-37 (G29AIIGLMVG37), which comprises nine residues (referred to as peptide **P1** in Table 1), served as the foundation sequence for designing destabilizers targeting the Aβ42 protofibril. This selection is supported by previous research findings. For example, studies have demonstrated that poly-N methylated hexapeptides derived from the Aβ32-37 sequence located at the C-terminus of Aβ can inhibit β-sheets accumulation and fibril formation, as well as reduce Aβ toxicity under laboratory conditions [25]. Additionally, Kaminker *et al.* observed that the N-methylated derivatives exhibit superior protease resistance compared to other alkyl substitutions [26]. Hydrophobic interactions are recognized as key drivers of protein folding, with hydrophobic residues playing a crucial role in fibril stability [12,27,28]. Notably, the hydrophobic C-terminal region of Aβ has been identified as having a key role in its self-aggregation [29].

Table 1 presents the complete list of designed peptides. For peptides **P2** to **P9**, a single residue within the Aβ29-37 sequence has been N-methylated, while peptides **P31** to **P43** represent double and triple N-methylations. For all other peptides (**P10** to **P30**), single or multiple mutations have been made in the sequence, replacing amino acids with proline, phenylalanine, isobutyric acid (Aib), lysine, glutamic acid, and valine, as described in Table S1. These mutations have been demonstrated to disrupt the interactions that stabilize the fibril [27,29-31]. In the case of charged amino acids, it has been argued that the electrostatic repulsions induced by this type of mutation inhibit further growth of fibrils, while aromatic amino acids increase peptide-protofibril binding affinity. It should be noted that the N- and C-terminus of some peptides are modified with acetyl and amine groups, respectively.

Molecular Docking Studies

The Aβ42 protofibril structure was obtained from the Protein Data Bank (PDB ID:2BEG) [32] and polar hydrogen atoms were added to the structure. Molecular docking was performed using AutoDock 4 [33]. All input files were prepared using AutoDock Tools. Kollman and Gasteiger charges were added to the protofibril and peptides [34,35]. The grid maps were calculated using the grid spacing of 0.375 Å and grid box dimensions were set to 126 Å × 100 Å × 100 Å. The Aβ42 protofibril was chosen as a rigid structure, whereas the designed peptides were allowed to be flexible in the grid box. The Lamarckian Genetic Algorithm was employed for global search, while the Solis & Wets algorithm was used for local search [36,37].

Binding Free Energy Calculations

The best conformation in molecular docking for each Aβ42 protofibril-peptide complex was saved as an input file for a 20 ns simulation. After MD simulation, the binding free energy between Aβ42 protofibril and peptides was evaluated based on the molecular mechanics Poisson-Boltzmann surface area (MM-PBSA) method using the g_mmpbsa tool [38-39]. The binding free was calculated by employing the following equations:

Table 1. Sequences of the Peptides Designed

Peptide	Sequence	Peptide	Sequence
P1	H-GAIIGLMVG-NH_2	**P23**	H-GAI (Me-I)GLMPG-NH_2
P2	H-G(Me-A)IIGLMVG-NH_2	**P24**	H-GAI (Me-I)GLMFG-NH_2
P3	H-GA(Me-I)IGLMVG-NH_2	**P25**	H-GFI (Me-I)GLMFG-NH_2
P4	H-GAI(Me-I)GLMVG-NH_2	**P26**	H-GAII (Me-G)LMFG-NH_2
P5	H-GAII(Me-G)LMVG-NH_2	**P27**	H-GAIIG(Me-L) MFG-NH_2
P6	H-GAIIG(Me-L)MVG-NH_2	**P28**	H-GFIIG (Me-L)MFG-NH_2
P7	H-GAIIGL(Me-M)VG-NH_2	**P29**	H-GVIIG (Me-L)MVG-NH_2
P8	H-GAIIGLM(Me-V)G-NH_2	**P30**	H-GFIIGL(Me-M)FG-NH_2
P9	H-GAIIGLMV(Me-G)-NH_2	**P31**	H-GAII(Me-G)LMV(Me-G)-NH_2
P10	ACE-G(Me-I)IIGLMVV-NH_2	**P32**	H-GAII(Me-G)(Me-L)MVG-NH_2
P11	ACE-GA(Me-I)ILFFMG-NH_2	**P33**	ACE-GAI(Me-I)G(Me-L)MVG-NH_2
P12	ACE-G(Me-I)ILVFFME-NH_2	**P34**	ACE-GAIIG(Me-L)M(Me-V)G-NH_2
P13	H-GFIIGLM(Me-F)G-NH_2	**P35**	ACE-G(Me-A)I(Me-I)GLMVG-NH_2
P14	H-Aib(Me-I)IGAibMVG-NH_2	**P36**	ACE-GA(Me-I)IGLM(Me-V)G-NH_2
P15	H-GA(Me-I)IGLMPG-NH_2	**P37**	ACE-GA(Me-I)IG(Me-L)MVG-NH_2
P16	H-GA(Me-I)IGLMFG-NH_2	**P38**	ACE-GA(Me-I)I(Me-G)L(Me-M)VG-NH_2
P17	H-GA(Me-I)IGLMKK-NH_2	**P39**	ACE-GAI(Me-I)G(Me-L)M(Me-V)G-NH_2
P18	H-GA(Me-I)IFFMVG-NH_2	**P40**	ACE-G(Me-A)I(Me-I)G(Me-L)MVG-NH_2
P19	ACE-GA(Me-I)ILFFMV-NH_2	**P41**	ACE-GA(Me-I)IG(Me-L)M(Me-V)G-NH_2
P20	H-GF(Me-I)IGLMFG-NH_2	**P42**	ACE-(Me-G)A(Me-I)I(Me-G)LMVG-NH_2
P21	H-KA(Me-I)IGLMVK-NH_2	**P43**	ACE-GA(Me-I)IG(Me-L)(Me-M)VG-NH_2
P22	ACE-AibF(Me-I)IGLMFAib-NH_2		

$$\Delta G_{binding} = \Delta E_{MM} + \Delta G_{solv} \quad (1)$$

$$\Delta E_{MM} = \Delta E_{vdW} + \Delta E_{elec} \quad (2)$$

$$\Delta G_{solv} = \Delta G_{ps} + \Delta G_{nps} \quad (3)$$

In these expressions, ΔE_{MM} represents the molecular mechanics contribution to the binding free energy in a vacuum, which comprises the sum of van der Waals (ΔE_{vdW}) and electrostatic (ΔE_{elec}) contributions. Additionally, ΔG_{ps} and ΔG_{nps} denote the polar and non-polar contributions to the solvation-free energy (ΔG_{solv}), respectively. Non-polar solvation energy term was calculated by using the solvent-accessible surface area (SASA) model with a solvent radius of 1.4 Å.

Molecular Dynamics (MD) Simulations

MD simulations of the complex of Aβ42 protofibril with peptides were carried out using GROMACS 2020.6 software [40] and AMBER99SB-ILDN force field [41]. This force field has been used to simulate the structures of Aβ dimers and fibrils and is shown to be in agreement with experimental data [42,43]. All systems were solvated with a cubic box of TIP3P water [44], ensuring a minimum distance of 1.0 nm between the complex and the periodic box boundaries. Additionally, the systems were electrically neutralized by adding the appropriate number of sodium and chloride ions. Energy minimization of the systems was carried out for 5000 steps with the steepest descent algorithm. The systems were then equilibrated using an NVT simulation for 500 ps, followed by an NPT simulation of the same length. The

Berendsen thermostat [45] and the Parrinello-Rahman barostat [46] were used to maintain the temperature of 310 K and the pressure of 1 bar, respectively. The linear constraint solver (LINCS) algorithm [47] with an integration time step of 1 fs was applied to constrain the lengths of all bonds. The particle mesh Ewald (PME) method [48] was used to calculate the long-range electrostatic interactions, and the cutoff for short-range van der Waals interactions was kept at 1.0 nm. Short MD simulations (20 ns) and more extensive MD simulations (100 ns sampling time) were carried out in explicit water. The MD trajectories were analyzed using GROMACS tools [40].

RESULTS AND DISCUSSION

Molecular Docking and Binding Free Energy Calculations

In this study, molecular docking was employed to create molecular models of peptide-protofibril complexes for subsequent calculations. Table S2 lists the binding energies calculated from molecular docking. The figures in this Table show that approximately half of the peptides interact with the lateral region of the Aβ protofibril, which can inhibit fibril growth [49]. The subsequent aggregation of the Aβ peptides to fibrils is important for the development of the disease. The free energy of binding for the complexes was subsequently evaluated using the MM-PBSA method, and the results are reported in Table S3. Table 2 presents the binding free energy values for a subset of six complexes that were selected for further MD simulations. The binding free energy of peptides varies between -44.9 and -729.2 kJ mol^{-1}. MM-PBSA results show that the values of electrostatic and van der Waals energy contributions are greater than the free energy of nonpolar solvation, indicating that both electrostatic and van der Waals interactions are the effective forces between peptides and Aβ42 protofibril. Meanwhile, electrostatic interactions have a greater contribution to the binding free energy. The role of electrostatic interactions in fibril arrangement is demonstrated before [50]. When such interactions are lost, Aβ42 protofibril fibrillation can be disrupted. Based on the binding energy results, several peptides were selected for further investigation using 100 ns MD simulations. Since the docking score and binding free energy of peptide **P1** were low, the 100 ns simulation was not performed for it.

MD Simulations of Aβ42 Protofibril-peptide Complexes

Effect of peptides on the structural characteristics of Aβ42 protofibril. The purpose of this study is to investigate the destabilizing effect of N-methylated peptides on the structure of Aβ42 protofibrils. MD simulations of designed peptides with Aβ protofibril were performed to observe the structural changes and stability of Aβ42 protofibril. Snapshots of the systems were taken during the simulation at 0, 50, and 100 ns. Figure 1 demonstrates that Aβ42 protofibril-peptide complexes exhibit reduced β-sheet content compared to the reference structure (Aβ42 protofibril) throughout the simulation. Conversely, they show a higher content of random coil structures, resulting in decreased structural stability within the protofibril. The decrease in β-sheet content is especially notable in certain complexes, such as **P3**, **P11**, and **P13**.

Table 2. Binding Free Energy between Aβ42 Protofibril and Various Peptides from MM-PBSA Calculations

Model System	Binding energy (kJ mol^{-1})	van der Waals energy (kJ mol^{-1})	Electrostatic energy (kJ mol^{-1})	Polar solvation energy (kJ mol^{-1})	Non-polar solvation energy (kJ mol^{-1})
Protofibril –**P3**	-602.5 ± 5.5	-163.6 ± 1.9	-686.9 ± 6.3	267.2 ± 3.3	-20.3 ± 0.2
Protofibril –**P10**	-110 ± 1.2	-156.2 ± 1.2	-12.7 ± 0.7	80.03 ± 0.7	-21 ± 0.1
Protofibril –**P11**	-530.1 ± 5.1	-181.4 ± 2.3	-534.5 ± 5.7	208.1 ± 3.3	-22.5 ± 0.2
Protofibril –**P13**	-683.9 ± 7.7	-66.3 ± 1	-956.5 ± 12.2	349.8 ± 5.6	-10.6 ± 0.1
Protofibril –**P18**	-56.6 ± 1.2	-126.3 ± 1.2	5.79 ± 0.3	79 ± 1	-15 ± 0.1
Protofibril –**P24**	-528.4 ± 3.5	-147.7 ± 1.1	-597.2 ± 6.6	235.3 ± 4	-18.9 ± 0.1

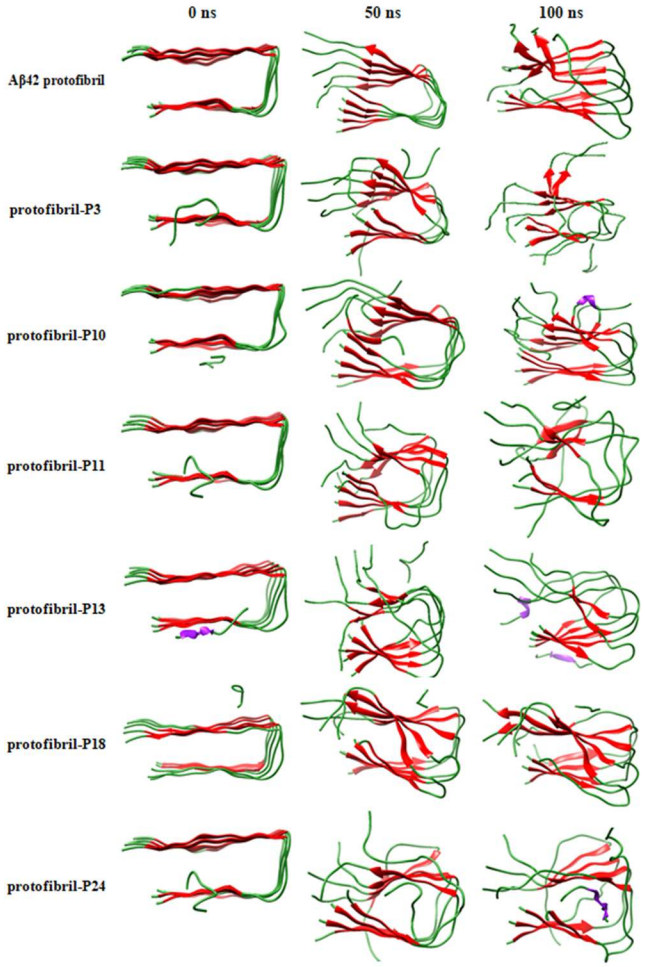

Fig. 1. Snapshots of Aβ42 protofibril-peptide complexes during the simulation. Helices are shown in purple, coils in green, and strands in red.

To investigate the temporal evolution of the structural stability of Aβ42 protofibrils, RMSD analysis was performed for Aβ42 protofibrils and Aβ42 protofibril-peptide complexes over trajectories of 100 ns (Fig. 2A). Table 3 presents the average RMSD values for these systems, which are higher for all complexes compared to the value for the Aβ42 protofibril (0.62 nm), indicating destabilizing effects of ligands on the protofibril. Among different peptides tested, peptide **P3** demonstrates the most remarkable effect on the protofibril, with an increase in RMSD to 0.85 nm (as depicted by the red-colored curve in Fig. 2A). Additionally, complexes containing peptides **P10** and **P11** show large fluctuations during the last 20 ns of the simulation. Nevertheless, the RMSD for all the systems reaches a plateau at the end of simulations, indicating equilibrium conditions for the trajectories. Also, the RMSD of different chains of the protofibril in the **P11** and **P3** complexes (Fig. S1) shows that the edge chains have relatively higher levels of disruption compared to the rest of the chains.

Another important parameter calculated is the radius of gyration (R_g) which can provide a measure of the compactness of a molecular structure. Higher values of R_g indicate a less compact structure. Figure 2B shows the variation of R_g with time for the protofibril and complexes, and the average values are listed in Table 3. In line with the results of RMSD analysis, Aβ42 protofibril-peptide complexes show a slightly increased R_g in comparison to the protofibril, and peptide **P3** shows the most favorable potential for disturbing the protofibril structure into a less compact form.

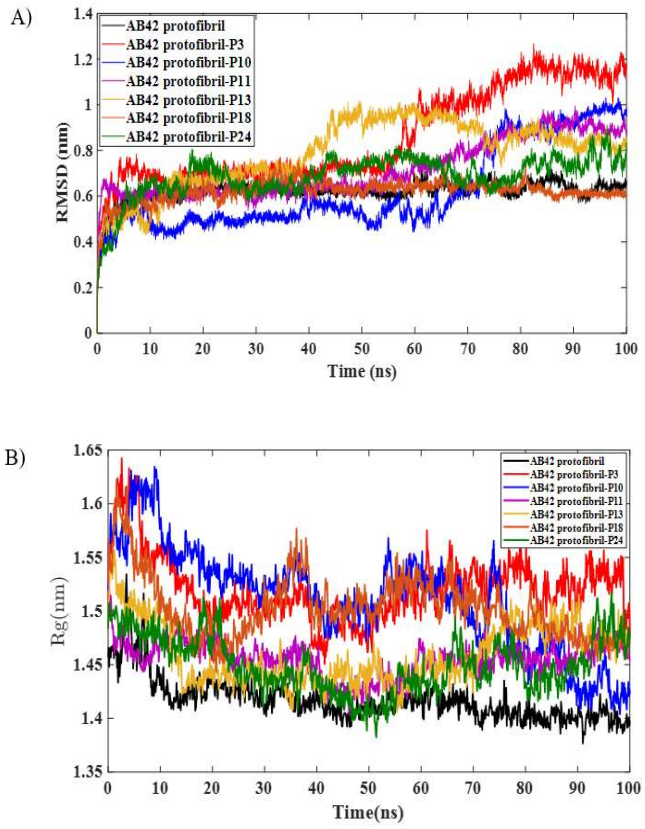

Fig. 2. Variation of RMSD (A) and Rg (B) values with time for the simulated systems.

Table 3. Averaged Rg and RMSD Values for Aβ42 Protofibril-peptides Systems During 100 ns Simulations

Model system	Average Rg	Average RMSD
Aβ42 Protofibril	1.41	0.62
Aβ42 Protofibril – **P3**	1.52	0.85
Aβ42 Protofibril – **P10**	1.51	0.62
Aβ42 Protofibril – **P11**	1.45	0.71
Aβ42 Protofibril – **P13**	1.46	0.78
Aβ42 Protofibril – **P18**	1.50	0.62
Aβ42 Protofibril – **P24**	1.44	0.68

Table 4. The Secondary Structure Component Statistics for Aβ42 Protofibril-peptides Complexes

Model system	Coil	β-Structure[a]	Bend	Turn
Aβ42 Protofibril	33	54	9	1
Aβ42 Protofibril – **P3**	39	43	12	3
Aβ42 Protofibril – **P10**	41	44	11	1
Aβ42 Protofibril – **P11**	46	34	13	3
Aβ42 Protofibril – **P13**	42	42	9	4
Aβ42 Protofibril – **P18**	38	46	11	2
Aβ42 Protofibril – **P24**	42	41	12	3

[a]β-Structure is the sum of β-sheet and β-bridge

As previously mentioned, Aβ fibrils are formed in the path of the Aβ accumulation mechanism and before the formation of neural plaques. Therefore, inhibitors that change and rebuild the structure of Aβ fibrils are effective in the treatment of AD. The stability of proteins is related to their ability to obtain defined and ordered secondary structures, which can be checked with the help of secondary structure analysis [51]. To gain quantitative insight into these changes, DSSP analysis was performed to follow the secondary structure during simulations (Tables 4 and S4). The secondary structure content for the Aβ42 protofibril in the present study is almost identical to that reported by Kaur *et al.* [12]. Due to the significant increase of coil value in peptide **P11**, its β-sheet has the lowest value compared to the reference. The critical factor affecting the stability of the Aβ42 protofibril is its elevated β-sheet content. Across all protofibril-peptide systems investigated, a decline in β-sheet content and a corresponding rise in coil structure are evident. The inclusion of N-methylated peptides in the interaction with Aβ42 protofibril has led to a reduction in the number of residues contributing to the β-sheet structure, consequently reverting them to the coil conformation.

Destabilization of Aβ42 Protofibril by Peptides

The interactions among β-sheets within the structure of the Aβ42 are crucial for maintaining the stability of its secondary structure and facilitating protein folding and unfolding processes. Specifically, hydrogen bonds between β-sheets represent one of the most significant types of interactions. The biological function of a protein can be modulated by the loss or gain of even a weak hydrogen bond [24,52]. We have therefore evaluated the number of total hydrogen bonds between protofibril chains, as well as between protofibril and designed peptides for all systems simulated. Figure 3 depicts the plots showing the time variation of the average total number of hydrogen bonds within the protofibril for these systems. The presence of peptides significantly reduces the number of hydrogen bonds within the protofibril, ranging from 58.49 to 69.23, compared to 77.72 for the reference structure (protofibril alone). The most significant decrease is observed for the peptide **P11**, indicating a pronounced protofibril destabilization induced by this peptide. In the study conducted on the destabilization effects of caffeine on the Aβ42 protofibril, the number of hydrogen bonds in the protofibril structure was reduced from 71.9 to 56.5, which suggests a disruption of hydrogen bonds in the presence of caffeine [51].

The average number of total hydrogen bonds accumulated per frame of the trajectory during the simulation between Aβ42 protofibril and peptides in the complexes is shown in Fig. 4A. For all six complexes studied, the peptide established hydrogen bond interactions with the protofibril, the maximum number of hydrogen bonds being for **P3**, **P10**, and **P11** and the minimum for **P18**. Table S5 presents the characteristics of these hydrogen bonds, including donor (D) and acceptor (A) groups as well as D…A distance at the end of simulations. The Phe19, Leu34, Met35, Ile41, and Val36

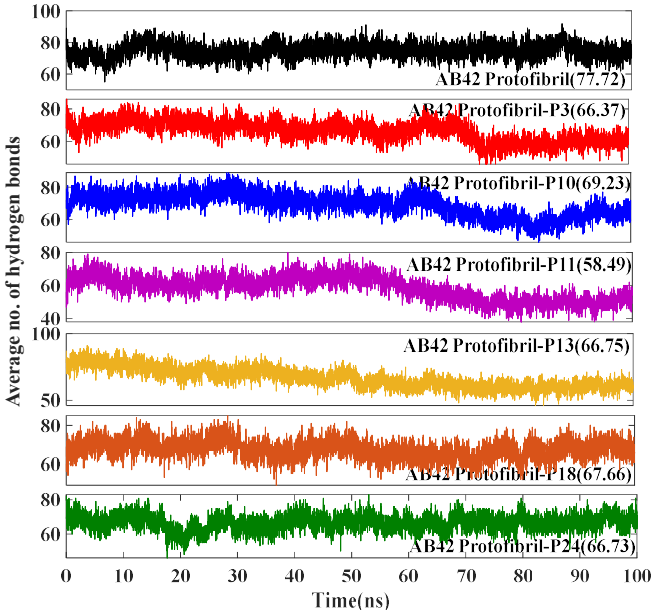

Fig. 3. The average number of hydrogen bonds between Aβ42 protofibril and peptides during simulation.

Residues participate in the formation of hydrogen bond with Aβ protofibril. These residues played a key role in binding REF to Aβ fibrils in the study by Gupta and Dasmahapatra [53].

The hydrogen atoms of the main chain residues Val8 of the peptide **P3**, Leu34, and Val36 of the protofibril (chain A) form hydrogen bonds with the oxygen atoms of the main chain residues Leu34 of the protofibril, Leu6, and Val8 of the peptide **P3** (with distances of 3.16 Å, 2.72 Å, and 3.03 Å, respectively) (Figure 4B). The effective residue in the self-assembly of [54] Aβ of the peptide **P11** forms a hydrogen bond with the oxygen atom of the Met35 residue of the protofibril (chain C) at a distance of 3.09 Å (Fig. 4C). The hydrophobic residue of Met35 can play a role in the pathogenesis of AD due to putative interactions in biological systems. It has been shown that the binding site of this residue can be effective in inhibiting PPIs and preventing amyloid fibril formation [55].

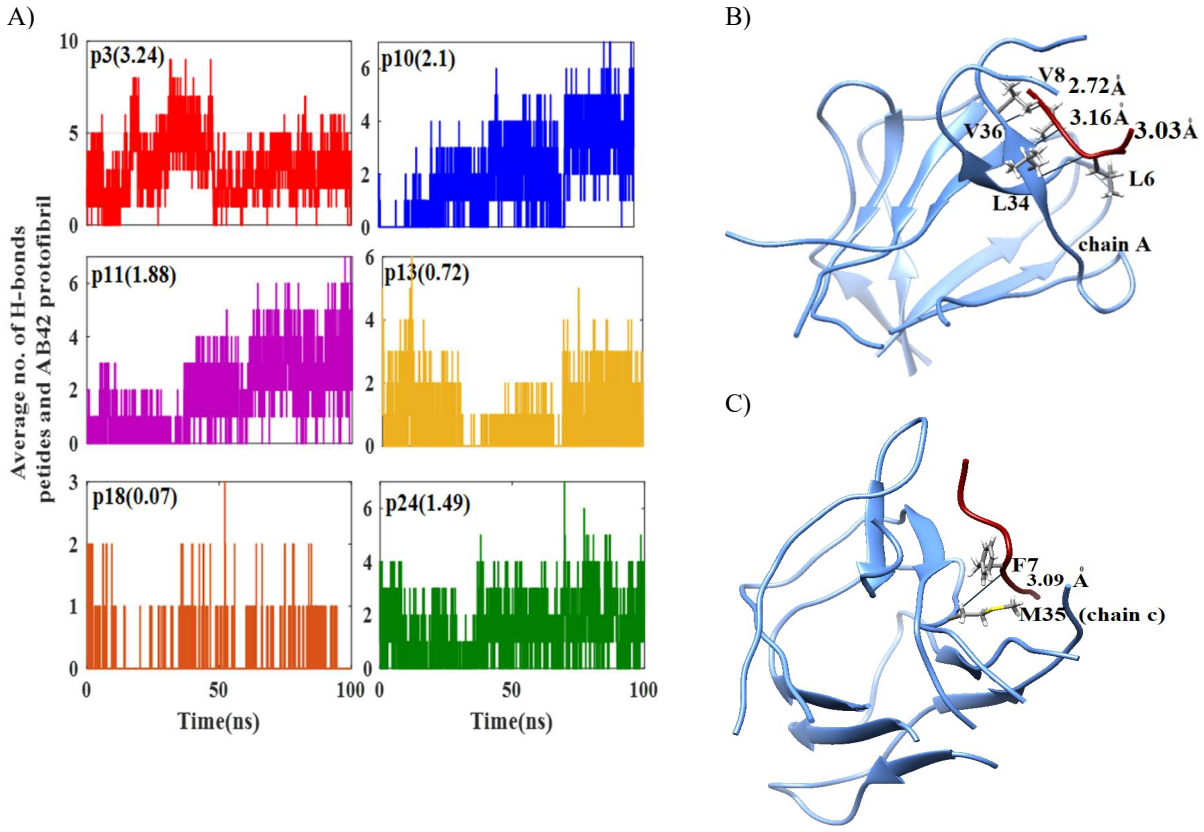

Fig. 4. The average number of total hydrogen bonds during simulation in $A\beta_{42}$ protofibril and $A\beta_{42}$ protofibril-peptides complexes (A), and snapshots from protofibril complex with **P3** (B) and **P11** (C) showing hydrogen bonds.

he formation of two hydrogen bonds of the **P3** peptide with the Val36 residue of the protofibril (Tables S5) probably influenced the interaction between the two hydrophobic amino acids Ala21 and Val36, which play an important role in the stability and compression of the two β-sheets in the U-shaped form of the protofibril. The distance between two hydrophobic amino acids, Ala21 and Val36, has been measured between the A-B and D-E chains of the protofibril (Tables S6). This distance is observed to change more in the **P3** peptide complex compared to the reference structure. The participation of hydrophobic amino acids of protofibril in the formation of hydrogen bonds with peptides is effective in destabilizing hydrophobic interactions.

We have also analyzed the salt bridge interactions between oppositely charged ions, another category of stabilizing interactions that facilitate the growth of the protofibril. The salt bridge formed between the Asp23 and Lys28 sidechains is particularly noteworthy. For this purpose, the distribution of the salt bridge interaction distance between the carbon atom of the carboxyl group (Cγ) of the Asp23 residue and the nitrogen atom of the NH_3^+ group (Nζ) of the Lys28 residue of the chains was evaluated in the Aβ42 protofibril alone and the presence of peptides [56,57]. A salt bridge is formed when this distance is less than 0.46 nm [58]. Since Aβ42 peptides tend to bind to the A chain or the E chain of the protofibril, we calculated the salt bridge distances for chains A and B, as well as chains D and E. Figure 5 shows the distribution of the salt bridge distance between chains A and B for the systems. For the reference structure, the average salt bridge distance between the B and A chains is around 0.35 nm. The **P3** complex has two distance peaks: between 0.2 and 0.3 nm for 72% of the conformations and between 0.6 and 0.9 nm for 20%.

In the **P10** complex, 28% of the population have a distance of about 0.35 nm, 25% have a distance between 0.5 and 0.7 nm, and about 25% have a distance between 0.7 and 0.9 nm. A bimodal distribution was observed for the **P11** complex, whose dominant peak changes with a distance of about 1.3 to 1.4 nm. In the **P13** complex, two dominant peaks are observed, one with conformations at 1.55 nm and the other at 1.65 nm. In the **P18** complex (Fig. S2), 42% of the population distribution was in the range of 0.3 to 0.4 nm and, 30% was in the range of 0.5 to 0.7 nm. In the **P24** complex, three regions were observed, one with conformations with a distance of around 0.35 nm and two others with a distance of 0.55 and 0.85 nm.

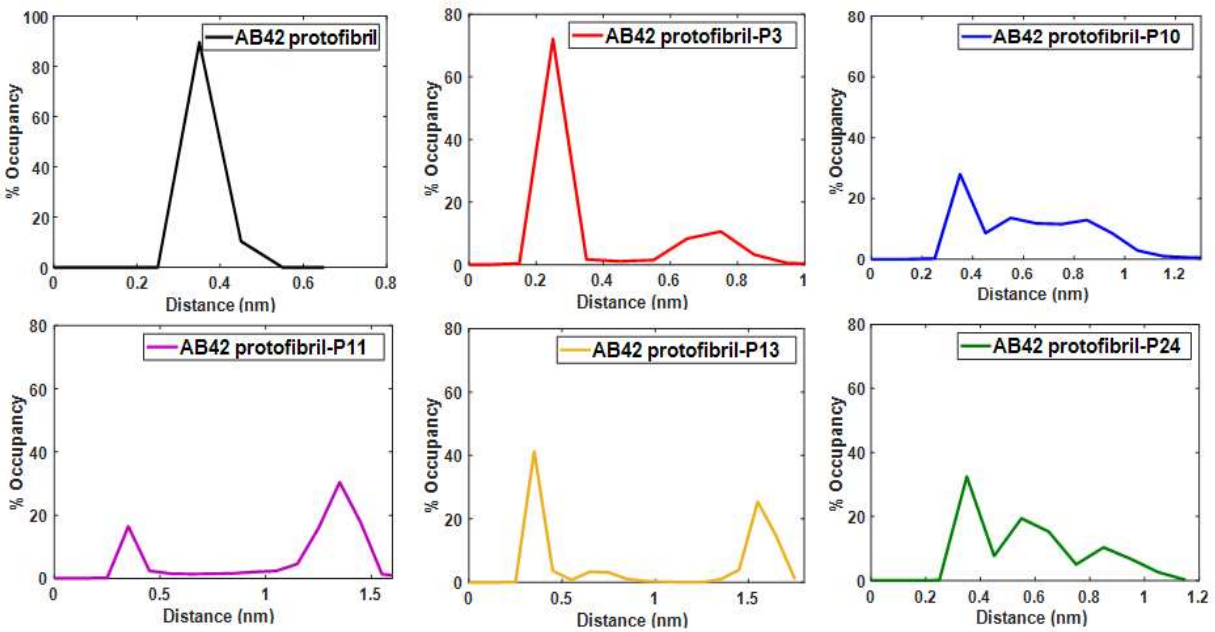

Fig. 5. Distance distributions between ASP23 (chain A) and LYS28 (chain B) residues for salt bridge formation in Aβ42 protofibril structure and Aβ42 protofibril-peptide complexes.

The distribution of salt bridge interaction distance between chain D and chain E was also investigated for all systems and shown in Fig S3. In all protofibril-peptide complexes, the measured distance increased. From the calculation of the salt bridge distance, it can be concluded that the presence of peptides can destabilize the salt bridge interactions in the Aβ42 protofibril. The details of the salt bridge interaction between A-B and D-E chains in **P3** and **P11** complexes are shown in Fig. 6.

The distance matrices, which contain the smallest distances between pairs of residues, were calculated and visualized using 2D contact maps. A contact map is a 2D derivative of the 3D structure of proteins, containing various residue-residue contacts within the structure. The pair of residues were considered to be in contact whenever the distance between them was less than 1.5 nm. Residue-residue contact maps of Aβ42 protofibril in the absence and presence of peptides were evaluated, and the results for the last 20 ns of MD simulations are plotted in Fig. 7. Closer contact of residues is observed in the reference structure, and in the complexes, it is altered. We observe a decrease in contact between residues, especially in peptide complexes **P3** and **P11**. An increase in the distance and a decrease in the contact between the Aβ42 protofibril residues indicate the instability of the protofibril structure.

It was also observed in the present work, the presence of peptides has led to a decrease in the content of the protofibril beta structure and an increase in the coil structure. Additionally, disruption of salt bridges and reduction of the number of interchain hydrogen bonds show the instability of protofibril in interaction with peptides.

CONCLUSION

In this work, we investigated the destabilizing effects of designed N-methylated peptides on the Aβ42 protofibril structure. The increase in the RMSD and Rg values and the decrease in the β-sheet content in the secondary structure analysis in the protofibril structure showed that the peptides have reduced the stability of the Aβ42 protofibril structure. Peptides **P3** and **P11** have better destabilizing potential as inhibitors of protofibril structure. The RMSD diagram of the different chains of the protofibril structure in these two peptide complexes shows that the edge chains show a higher level of disruption compared to the rest of the chains of the structure. This is effective in preventing the subsequent binding of Aβ peptide monomers to protofibril. By changing and modifying the peptide sequence and placing other amino acids in the peptide sequence, the destabilization potential of peptides, a therapeutic option, can be investigated as an inhibitor of Aβ protofibril aggregation.

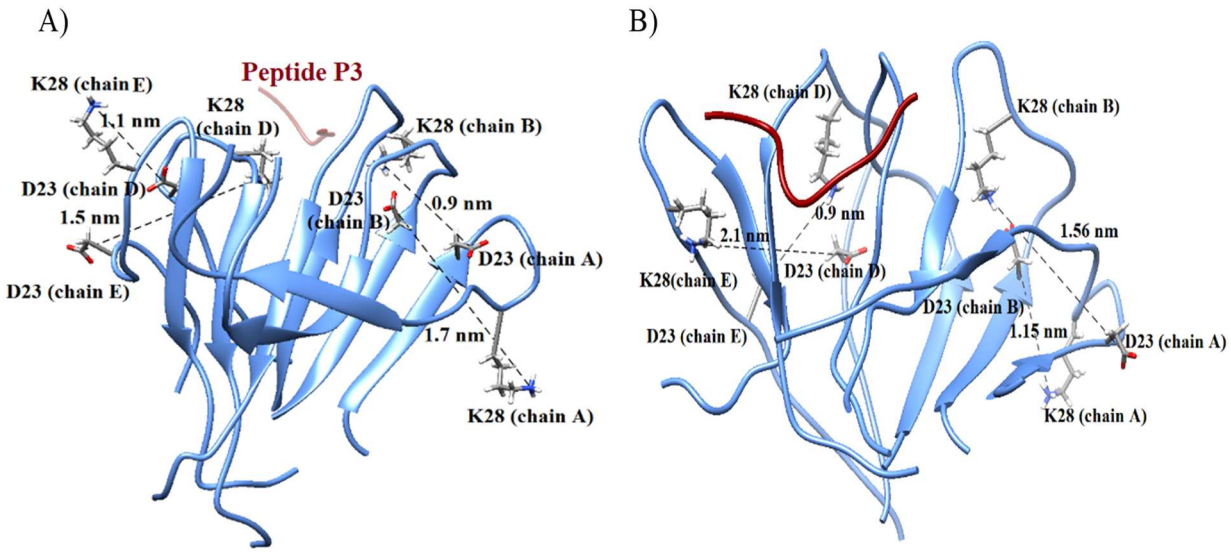

Fig. 6. Snapshots showing salt bridge interactions between Asp23 and Lys28 in Aβ42 protofibril complexes with **P3** (A) and **P11** (B). Peptide **P11** is marked in dark red in panel B.

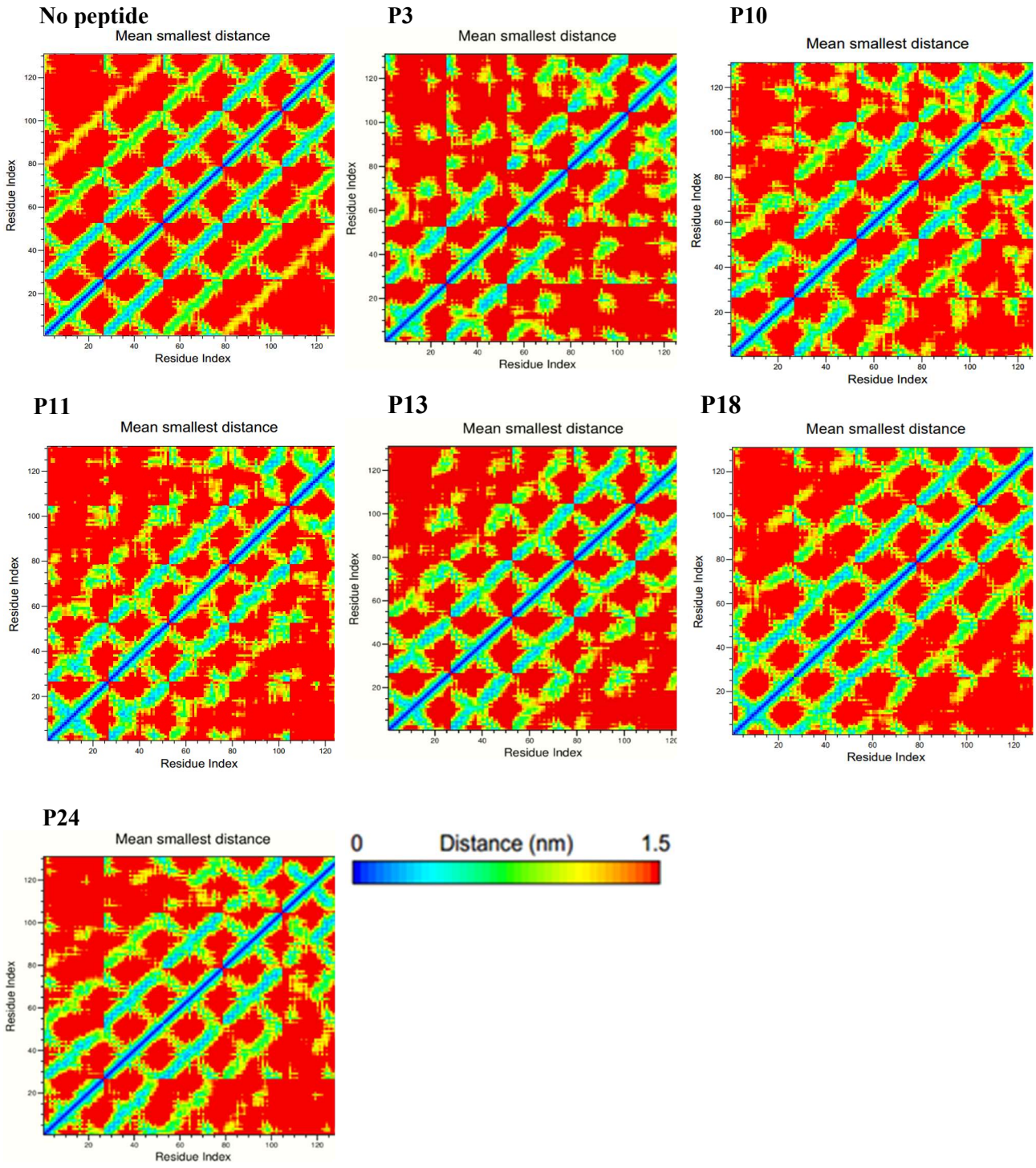

Fig. 7. The residue-residue contact maps for Aβ42 protofibril in the systems studied.

REFERENCES

[1] Kumar, A.; Singh, A., Ekavali. A review on Alzheimer's disease pathophysiology and its management: An update. *Pharmacol. Reports* **2015**, *67*, 195-203. https://doi.org/10.1016/j.pharep.2014.09.004.

[2] Rajasekhar, K.; Chakrabarti, M.; Govindaraju, T., Function and toxicity of amyloid beta and recent therapeutic interventions targeting amyloid beta in Alzheimer's disease. *Chem. Commun.* **2015**, *51*, 13434-50. https://doi.org/10.1039/c5cc05264e.

[3] Šimić, G.; Babić Leko, M.; Wray, S.; Harrington, C.; Delalle, I.; Jovanov-Milošević, N., *et al.* Tau protein hyperphosphorylation and aggregation in alzheimer's disease and other tauopathies, and possible neuroprotective strategies. *Biomolecules* **2016**, *6*, 2-28. https://doi.org/10.3390/biom6010006.

[4] Goyal, D.; Shuaib, S.; Mann, S.; Goyal, B., Rationally Designed Peptides and Peptidomimetics as Inhibitors of Amyloid-β (Aβ) Aggregation: Potential Therapeutics of Alzheimer's Disease. *ACS Comb. Sci.* **2017**, *19*, 55-80. https://doi.org/10.1021/acscombsci.6b00116.

[5] Jokar, S.; Erfani, M.; Bavi, O.; Khazaei, S.; Sharifzadeh, M.; Hajiramezanali, M.; *et al.* Design of peptide-based inhibitor agent against amyloid-β aggregation: Molecular docking, synthesis and in vitro evaluation. *Bioorg. Chem.* **2020**, *102*, 104050. https://doi.org/10.1016/j.bioorg.2020.104050.

[6] Alanazi, F. K.; Radwan, A. A.; Aou-Auda, H., Molecular scaffold and biological activities of anti-Alzheimer agents. *Trop. J. Pharm. Res.* **2022**, *21*, 439-51. https://doi.org/10.4314/tjpr.v21i2.30.

[7] Matuszyk, M. M.; Garwood, C. J.; Ferraiuolo, L.; Simpson, J. E.; Staniforth, R. A.; Wharton, S. B., Biological and methodological complexities of beta-amyloid peptide: Implications for Alzheimer's disease research. *J. Neurochem.* **2022**, *160*, 434-53. https://doi.org/10.1111/jnc.15538.

[8] Pardo-Moreno, T.; González-Acedo, A.; Rivas-Domínguez, A.; García-Morales, V.; García-Cozar, F. J.; Ramos-Rodríguez, J. J., *et al.* Therapeutic Approach to Alzheimer's Disease: Current Treatments and New Perspectives. *Pharmaceutics* **2022**, *14*, 1117. https://doi.org/10.3390/pharmaceutics14061117.

[9] Jalili, S.; Pakzadiyan, A., Tensile strain as an efficient way to tune transport properties of Graphdiyne/Borophene hetero-bilayers; a first principle investigation. *Comput. Mater. Sci.* **2023**, *224*, 112161. https://doi.org/10.1016/j.commatsci.2023.112161.

[10] Jokar, S.; Khazaei, S.; Gameshgoli, X. E.; Khafaji, M.; Yarani, B.; Sharifzadeh, M., *et al.* Amyloid ß-Targeted Inhibitory Peptides for Alzheimer's Disease: Current State and Future Perspectives. *Alzheimer's Dis. Drug Discov.* **2020**, 51-68. https://doi.org/10.36255/exonpublications.alzheimersdisease.2020.ch3.

[11] Yang, A.; Li, X.; Li, D.; Zhang, M.; Du, H.; Li, C., *et al.* Observation of molecular inhibition and binding structures of amyloid peptides. *Nanoscale* **2012**, *4*, 1895-909. https://doi.org/10.1039/c2nr11508e.

[12] Kaur, A.; Kaur, A.; Goyal, D.; Goyal, B., How Does the Mono-Triazole Derivative Modulate Aβ42Aggregation and Disrupt a Protofibril Structure: Insights from Molecular Dynamics Simulations. *ACS Omega* **2020**, *5*, 15606-19. https://doi.org/10.1021/acsomega.0c01825.

[13] Kanchi, P. K.; Dasmahapatra, A. K., Destabilization of the Alzheimer's amyloid-β peptide by a proline-rich β-sheet breaker peptide: a molecular dynamics simulation study. *J. Mol. Model.* **2021**, *27*, 107471. https://doi.org/10.1007/s00894-021-04968-x.

[14] Mitra, A.; Sarkar, N., Sequence and structure-based peptides as potent amyloid inhibitors: A review. *Arch. Biochem. Biophys.* **2020**, *695*, 108614. https://doi.org/10.1016/j.abb.2020.108614.

[15] Tillett, K. C.; Del Valle, J. R., N -Amino peptide scanning reveals inhibitors of Aβ42 aggregation. *RSC Adv.* **2020**, *10*, 14331-6. https://doi.org/10.1039/d0ra02009e.

[16] Laxio Arenas, J.; Kaffy, J.; Ongeri, S., Peptides and peptidomimetics as inhibitors of protein–protein interactions involving β-sheet secondary structures. *Curr. Opin. Chem. Biol.* **2019**, *52*, 157-67.

https://doi.org/10.1016/j.cbpa.2019.07.008.

[17] Eskici, G.; Gur, M., Computational Design of New Peptide Inhibitors for Amyloid Beta (Aβ) Aggregation in Alzheimer's Disease: Application of a Novel Methodology. *PLoS One* **2013**, *8*, e66178. https://doi.org/10.1371/journal.pone.0066178.

[18] Ban, T.; Hoshino, M.; Takahashi, S.; Hamada, D.; Hasegawa, K.; Naiki, H., *et al.* Direct observation of Aβ amyloid fibril growth and inhibition. *J. Mol. Biol.* **2004**, *344*, 757-67. https://doi.org/10.1016/j.jmb.2004.09.078.

[19] Kokkoni, N.; Stott, K.; Amijee, H.; Mason, J. M.; Doig, A. J., N-methylated peptide inhibitors of β-amyloid aggregation and toxicity. Optimization of the inhibitor structure. *Biochemistry* **2006**, *45*, 9906-18. https://doi.org/10.1021/bi060837s.

[20] Sciarretta, K. L.; Boire, A.; Gordon, D. J.; Meredith, S. C., Spatial separation of β-sheet domains of β-amyloid: Disruption of each β-sheet by N-methyl amino acids. *Biochemistry* **2006**, *45*, 9485-95. https://doi.org/10.1021/bi0605585.

[21] Bose, P. P.; Chatterjee, U.; Hubatsch, I.; Artursson, P.; Govender, T.; Kruger, H. G., *et al. In vitro* ADMET and physicochemical investigations of poly-N-methylated peptides designed to inhibit Aβ aggregation. *Bioorganic Med. Chem.* **2010**, *18*, 5896-902. https://doi.org/10.1016/j.bmc.2010.06.087.

[22] Hiramatsu, H.; Ochiai, H.; Komuro, T., Effects of N-Methylated Amyloid- β 30-40 Peptides on the Fibrillation of Amyloid- β 1-40. *Chem. Biol. Drug Des.* **2016**, *87*, 425-33. https://doi.org/10.1111/cbdd.12674.

[23] Doig, A. J.; Hughes, E.; Burke, R. M.; Su, T. J.; Heenan, R. K.; Lu, J., Inhibition of toxicity and protofibril formation in the amyloid-beta peptide beta(25-35) using N-methylated derivatives. *Biochem. Soc. Trans* **2002**, *30*, 537-42. https://doi.org/10.1042/bst0300537.

[24] Schwarze, B.; Korn, A.; Höfling, C.; Zeitschel, U.; Krueger, M.; Roßner, S., *et al.* Peptide backbone modifications of amyloid β (1-40) impact fibrillation behavior and neuronal toxicity. *Sci. Rep.* **2021**, *11*, 23767. https://doi.org/10.1038/s41598-021-03091-4.

[25] Bose, P. P.; Chatterjee, U.; Nerelius, C.; Govender, T.; Norström, T.; Gogoll, A., *et al.* Poly-N-methylated amyloid β-peptide (Aβ) C-terminal fragments reduce Aβ toxicity in vitro and in Drosophila melanogaster. *J. Med. Chem.* **2009**, *52*, 8002-9. https://doi.org/10.1021/jm901092h.

[26] Kaminker, R.; Anastasaki, A.; Gutekunst, W. R.; Luo, Y.; Lee, S. H.; Hawker, C. J., Tuning of protease resistance in oligopeptides through: N-alkylation. *Chem. Commun.* **2018**, *54*, 9631-4. https://doi.org/10.1039/c8cc04407d.

[27] Adewole, K. E.; Gyebi, G. A.; Ibrahim, I. M., Amyloid β fibrils disruption by kolaviron: Molecular docking and extended molecular dynamics simulation studies. *Comput. Biol. Chem.* **2021**, *94*, 107557. https://doi.org/10.1016/j.compbiolchem.2021.107557.

[28] Kapadia, A.; Patel, A.; Sharma, K. K.; Maurya, I. K.; Singh, V.; Khullar, M., *et al*. Effect of C-terminus amidation of Aβ39-42fragment derived peptides as potential inhibitors of Aβ aggregation. *RSC Adv.* **2020**, *10*, 27137-51. https://doi.org/10.1039/d0ra04788k.

[29] Kaur, A.; Goyal, B., Identification of new pentapeptides as potential inhibitors of amyloid–β42 aggregation using virtual screening and molecular dynamics simulations. *J. Mol. Graph. Model.* **2023**, *124*, 108558. https://doi.org/10.1016/j.jmgm.2023.108558.

[30] Bett, C. K.; Serem, W. K.; Fontenot, K. R.; Hammer, R. P.; Garno, J. C., Effects of peptides derived from terminal modifications of the AB central hydrophobic core on AB fibrillization. *ACS Chem. Neurosci.* **2010**, *1*, 661-78. https://doi.org/10.1021/cn900019r.

[31] Esteras-Chopo, A.; Pastor, M. T.; Serrano, L.; López de la Paz, M., New Strategy for the Generation of Specific d-Peptide Amyloid Inhibitors. *J. Mol. Biol.* **2008**, *377*, 1372-81. https://doi.org/10.1016/j.jmb.2008.01.028.

[32] Lührs, T.; Ritter, C.; Adrian, M.; Riek-Loher, D.; Bohrmann, B.; Döbeli, H., *et al.* 3D structure of Alzheimer's amyloid-β (1-42) fibrils. *Proc. Natl. Acad. Sci.* **2005**, *102*, 17342-7.

[33] Steffen, C.; Thomas, K.; Huniar, U.; Hellweg, A.; Rubner, O.; Schroer, A., AutoDock4 and AutoDockTools4: Automated Docking with Selective Receptor Flexibility. *J. Comput. Chem.* **2010**, *31*, 2967-70.

[34] Jafar, J.; Mudalige, H.; Perera, O., Protein-ligand docking study for the identification of plant-based ligands and their binding sites against Alzheimer's disease **2023**.

[35] Roqanian, S.; Meratan, A. A.; Ahmadian, S.; Shafizadeh, M.; Ghasemi, A.; Karami, L., Polyphenols protect mitochondrial membrane against permeabilization induced by HEWL oligomers: Possible mechanism of action. *Int. J. Biol. Macromol.* **2017**, *103*, 709-20. https://doi.org/10.1016/j.ijbiomac.2017.05.130.

[36] Morris, G. M.; Goodsell, D. S.; Halliday, R. S.; Huey, R.; Hart, W. E.; Belew, R. K., *et al.* Automated docking using a Lamarckian genetic algorithm and an empirical binding free energy function. *J. Comput. Chem.* **1998**, *19*, 1639-62. https://doi.org/10.1002/(SICI)1096-987X(19981115)19:14<1639::AID-JCC10>3.0.CO;2-B.

[37] Huey, R.; Morris, G. M.; Olson, A. J.; Goodsell, D. S., Software news and update a semiempirical free energy force field with charge-based desolvation. *J. Comput. Chem.* **2007**, *28*, 1145-52. https://doi.org/10.1002/jcc.20634.

[38] Kumari, R.; Kumar, R.; Lynn, A., G-mmpbsa -A GROMACS tool for high-throughput MM-PBSA calculations. *J. Chem. Inf. Model.* **2014**, *54*, 1951-62. https://doi.org/10.1021/ci500020m.

[39] Genheden, S.; Ryde, U., The MM/PBSA and MM/GBSA methods to estimate ligand-binding affinities. *Expert. Opin. Drug Discov.* **2015**, *10*, 449-61.

[40] Van Der Spoel, D.; Lindahl, E.; Hess, B.; Groenhof, G.; Mark, A. E.; Berendsen, H. J. C., GROMACS: fast, flexible, and free. *J. Comput. Chem.* **2005**, *26*, 1701-18.

[41] Lindorff-Larsen, K.; Piana, S.; Palmo, K.; Maragakis, P.; Klepeis, J. L.; Dror, R. O., *et al.* Improved side-chain torsion potentials for the Amber ff99SB protein force field. *Proteins Struct. Funct. Bioinforma* **2010**, *78*, 1950-8. https://doi.org/10.1002/prot.22711.

[42] Man, V. H.; Nguyen, P. H.; Derreumaux, P., High-Resolution Structures of the Amyloid-β 1-42 Dimers from the Comparison of Four Atomistic Force Fields. *J. Phys. Chem. B* **2017**, *121*, 5977-87. https://doi.org/10.1021/acs.jpcb.7b04689.

[43] Kanchi, P. K.; Dasmahapatra, A. K., Enhancing the binding of the β-sheet breaker peptide LPFFD to the amyloid-β fibrils by aromatic modifications: A molecular dynamics simulation study. *Comput. Biol. Chem.* **2021**, *92*, 107471. https://doi.org/10.1016/j.compbiolchem.2021.107471.

[44] Jorgensen, W. L.; Chandrasekhar, J.; Madura, J. D.; Impey, R. W.; Klein, M. L., Comparison of simple potential functions for simulating liquid water. *J. Chem. Phys.* **1983**, *79*, 926-35. https://doi.org/10.1063/1.445869.

[45] Berendsen, H. J. C.; Postma, J. P. M.; Van Gunsteren, W. F.; Dinola, A.; Haak, J. R., Molecular dynamics with coupling to an external bath. *J. Chem. Phys.* **1984**, *81*, 3684-90. https://doi.org/10.1063/1.448118.

[46] Parrinello, M.; Rahman, A., Polymorphic transitions in single crystals: A new molecular dynamics method. *J. Appl. Phys.* **1981**, *52*, 7182-90. https://doi.org/10.1063/1.328693.

[47] Hess, B.; Bekker, H.; Berendsen, H. J. C., Fraaije JGEM. LINCS: A Linear Constraint Solver for molecular simulations. *J. Comput. Chem.* **1997**, *18*, 1463-72. https://doi.org/10.1002/(SICI)1096-987X(199709)18:12<1463::AID-JCC4>3.0.CO;2-H.

[48] York, D. M.; Darden, T. A.; Pedersen, L. G., The effect of long-range electrostatic interactions in simulations of macromolecular crystals: A comparison of the Ewald and truncated list methods. *J. Chem. Phys.* **1993**, *99*, 8345-8. https://doi.org/10.1063/1.465608.

[49] Verma, A.; Kumar, A.; Debnath, M., Molecular docking and simulation studies to give insight of surfactin amyloid interaction for destabilizing

Alzheimer's Aβ42 protofibrils. *Med. Chem. Res.* **2016**, *25*, 1616-22. https://doi.org/10.1007/s00044-016-1594-y.

[50] Barale, S. S.; Parulekar, R. S.; Fandilolu, P. M.; Dhanavade, M. J.; Sonawane, K. D., Molecular Insights into Destabilization of Alzheimer's Aβ Protofibril by Arginine Containing Short Peptides: A Molecular Modeling Approach. *ACS Omega* **2019**, *4*, 892-903. https://doi.org/10.1021/acsomega.8b02672.

[51] Gupta, S.; Dasmahapatra, A. K., Caffeine destabilizes preformed Aβ protofilaments: Insights from all atom molecular dynamics simulations. *Phys. Chem. Chem. Phys.* **2019**, *21*, 22067-80. https://doi.org/10.1039/c9cp04162a.

[52] Shuaib, S.; Narang, S. S.; Goyal, D.; Goyal, B., Computational design and evaluation of β-sheet breaker peptides for destabilizing Alzheimer's amyloid-β42 protofibrils. *J. Cell Biochem.* **2019**, *120*, 17935-50. https://doi.org/10.1002/jcb.29061.

[53] Gupta, S.; Dasmahapatra, A. K., Destabilization potential of phenolics on Aβ fibrils: Mechanistic insights from molecular dynamics simulation. *Phys. Chem. Chem. Phys.* **2020**, *22*, 19643-58. https://doi.org/10.1039/d0cp02459g.

[54] Marshall, K. E.; Morris, K. L.; Charlton, D.; O'Reilly, N.; Lewis, L.; Walden, H., *et al.* Hydrophobic, aromatic, and electrostatic interactions play a central role in amyloid fibril formation and stability. *Biochemistry* **2011**, *50*, 2061-71. https://doi.org/10.1021/bi101936c.

[55] Friedemann, M.; Helk, E.; Tiiman, A.; Zovo, K.; Palumaa, P.; Tõugu, V., Effect of methionine-35 oxidation on the aggregation of amyloid-β peptide. *Biochem. Biophys. Reports* **2015**, *3*, 94-9. https://doi.org/10.1016/j.bbrep.2015.07.017.

[56] Jani, V.; Sonavane, U.; Joshi, R., Destabilization potential of beta sheet breaker peptides on Abeta fibril structure: an insight from molecular dynamics simulation study. *RSC Adv.* **2021**, *11*, 23557-73. https://doi.org/10.1039/d1ra03609b.

[57] Saini, R. K.; Shuaib, S.; Goyal, B., Molecular insights into Aβ42 protofibril destabilization with a fluorinated compound D744: A molecular dynamics simulation study. *J. Mol. Recognit.* **2017**, *30*, e2656. https://doi.org/10.1002/jmr.2656.

[58] Linh, N. H.; Minh Thu, T. T.; Tu, L.; Hu, C. K.; Li, M. S., Impact of Mutations at C-Terminus on Structures and Dynamics of Aβ40 and Aβ42: A Molecular Simulation Study. *J. Phys. Chem. B* **2017**, *121*, 4341-54. https://doi.org/10.1021/acs.jpcb.6b12888.

[59] Soto, C.; Sigurdsson, E. M.; Morelli, L.; Kumar, R. A.; Castaño, E. M.; Frangione, B., β-sheet breaker peptides inhibit fibrillogenesis in a rat brain model of amyloidosis: Implications for Alzheimer's therapy. *Nat. Med.* **1998**, *4*, 822-6. https://doi.org/10.1038/nm0798-822.